LiDAR REMOTE SENSING & ORTHOPHOTO DATA COLLECTION

BATTLE CREEK • CALIFORNIA

10/31/2011

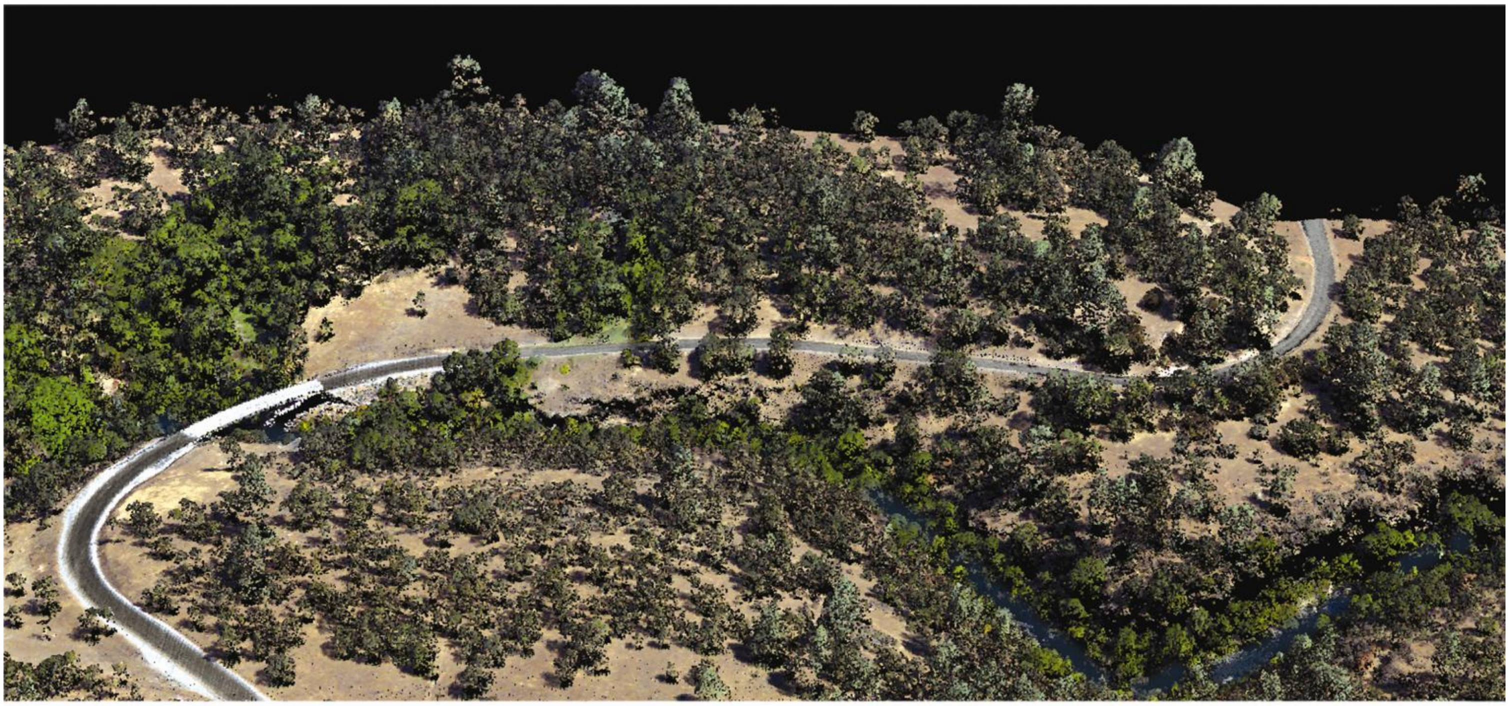

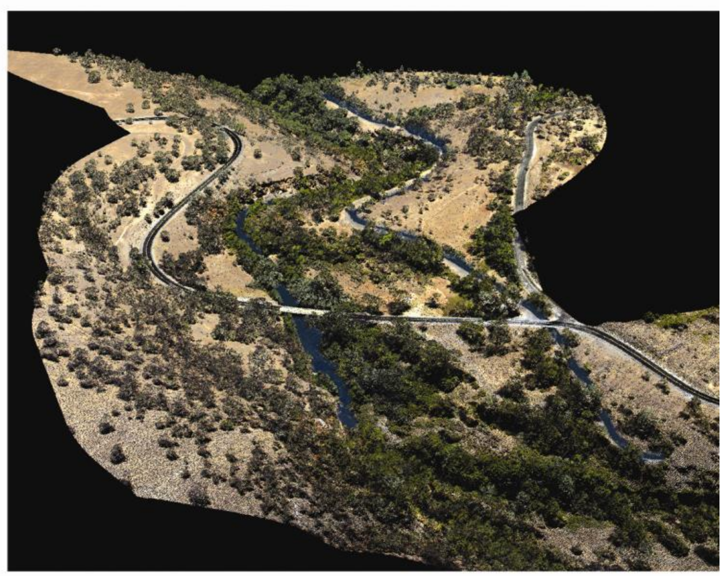

US FISH & WILDLIFE SERVICE

MATT BROWN - 10950 Tyler Road - Red Bluff, CA 96080

WATERSHED SCIENCES • 517 SW 2nd Street, Suite 400 - Corvallis, OR 97333

LiDAR Remote Sensing & True-Color Orthophotograph Data Collection:
Battle Creek, CA

TABLE OF CONTENTS

1. Overview

Watershed Sciences, Inc. (WSI) co-acquired Light Detection and Ranging (LiDAR) data and true-color orthophotographs of Battle Creek, CA. LiDAR and orthophotos were acquired on August 19th, 2011. This report documents the data acquisition, processing methods, accuracy assessment, and deliverables of that data. The requested area of 2,842 acres was expanded to include a 100m buffer to ensure complete coverage and adequate point densities around survey area boundaries, resulting in 6,528 acres of delivered LiDAR data and orthophotographs.

Figure 1. *Battle Creek, CA survey area*

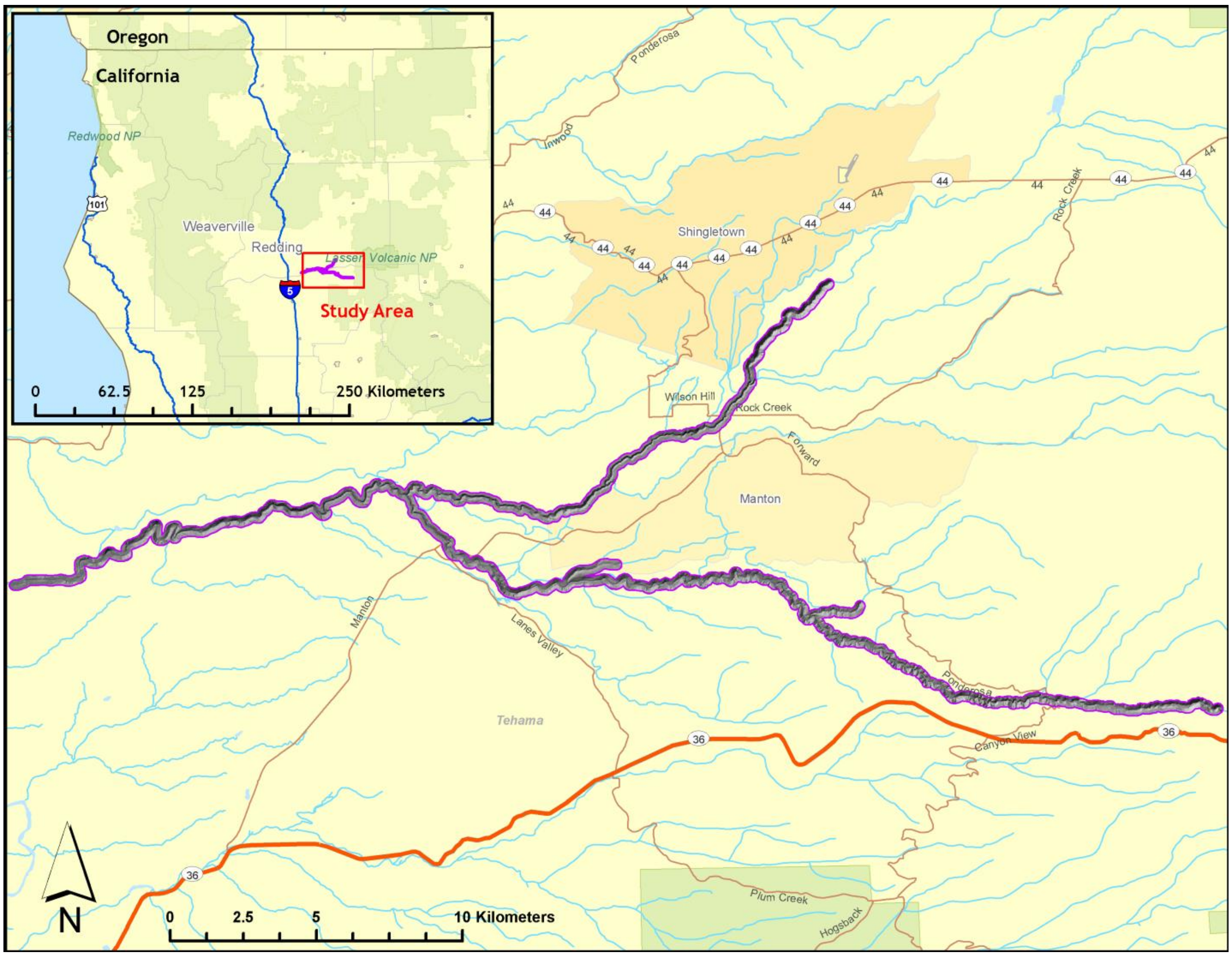

2. Acquisition

2.1 Airborne Survey – Instrumentation and Methods

The LiDAR survey utilized a ALS60 sensor in a Cessna Caravan 208B. The ALS60 sensor operates with Automatic Gain Control (AGC) for intensity correction. The Leica systems were set to acquire 105,900 laser pulses per second (i.e. 105.9 kHz pulse rate) and was flown at 900 meters above ground level (AGL), capturing a scan angle of ± 14^{o} from nadir. With these flight parameters, the laser swath width is 449m and the laser pulse footprint is 21cm. These settings were developed to yield points with an average native pulse density of ≥8 pulses per square meter over terrestrial surfaces. It is not uncommon for some types of surfaces (e.g. dense vegetation or water) to return fewer pulses than the laser originally emitted. These discrepancies between 'native' and 'delivered' density will vary depending on terrain, land cover, and the prevalence of water bodies.

The Cessna Caravan is a stable platform, ideal for flying slow and low for high density projects. The Leica ALS60 sensor head installed in the Caravan is shown on the right.

All areas surveyed with an opposing flight line side-lap of ≥60% (=100% overlap) to reduce laser shadowing and increase surface laser painting. The Leica ALS60 allows up to four range measurements (returns) per pulse, and all discernable laser returns were processed for the output dataset.

The aerial imagery was collected using a Leica RCD-105 39 megapixel digital camera. For the Battle Creek survey area, images were collected in 3 spectral bands (red, green, blue) with 60% along track overlap and 30% sidelap between frames. The acquisition flight parameters were designed to yield native pixel resolution of ≤20cm.

To accurately solve for laser point and photo position (geographic coordinates x, y, z), the positional coordinates of the airborne sensor and the attitude of the aircraft were recorded continuously throughout the LiDAR data collection mission. Aircraft position was measured twice per second (2 Hz) by an onboard differential GPS unit. Aircraft attitude was measured 200 times per second (200 Hz) as pitch, roll and yaw (heading) from an onboard inertial measurement unit (IMU). To allow for post-processing correction and calibration, aircraft/sensor position and attitude data are indexed by GPS time.

2.2 Ground Survey – Instrumentation and Methods

2.2.1 Monumentation

Watershed Sciences established two new monuments for this project. Monuments selected were found to have good visibility and optimal location to support a LiDAR acquisition flight. The Watershed Sciences' monumentation was done with 5/8" x 30" rebar topped with a metal cap stamped with "Watershed Sciences, Inc," the monument ID, and the year of establishment. Chris Yotter-Brown (OR-PLS #60438), Watershed Sciences' staff surveyor, provided professional supervision and oversight to all survey aspects of this project.

2.2.2 Control for Airborne Surveys

During the LiDAR survey, static (1 Hz recording frequency) ground surveys were conducted over set monuments. After the airborne survey, the static GPS data were processed using triangulation with Continuously Operating Reference Stations (CORS) and checked using the Online Positioning User Service (OPUS[1]) to quantify daily variance. Multiple sessions were acquired over the same monument to confirm antenna height measurements and reported position accuracy.

Trimble GPS equipment in the Battle Creek study area.

Indexed by time, these GPS data are used to correct the continuous onboard measurements of aircraft position recorded throughout the mission. Control monuments were located within 13 nautical miles of the survey area.

2.2.3. Instrumentation

All work was conducted using a Trimble GPS receiver model R7 with Zephyr Geodetic antenna with ground plane was deployed for all static control A Trimble model R8 GNSS unit was used for collecting check points using real time kinematic (RTK) survey techniques. For RTK data, the collector begins recording after remaining stationary for 5 seconds then calculating the pseudo range position from at least three epochs with the relative error under 1.5cm horizontal and 2cm vertical. All GPS measurements are made with dual frequency L1-L2 receivers with carrier-phase correction.

[1] Online Positioning User Service (OPUS) is run by the National Geodetic Survey to process corrected monument positions.

Table 1. Base Station control coordinates for the Battle Creek LiDAR data collection

Base Station ID	Datum: NAD83 (CORS96)		GRS80
	Latitude	Longitude	Ellipsoid Z (meters)
Battle_Cr_01	40° 24' 16.903"	121° 58' 35.396"	295.479
Battle_Cr_01	40° 26' 59.719"	121° 51' 46.656"	627.363
Battle_Cr_01	40° 26' 16.395"	121° 54' 52.651"	501.708

2.2.4. Methodology

Each aircraft is assigned a ground crew member with two Trimble R7 receivers and an R8 receiver. The ground crew vehicles are equipped with standard field survey supplies and equipment including safety materials. All control monuments were observed for a minimum of one survey session lasting no fewer than 6 hours and a second session lasting no fewer than 4 hours. At the beginning of every session the tripod and antenna were reset, resulting in two independent instrument heights and data files. Data was collected at a rate of 1Hz using a 10 degree mask on the antenna.

The ground crew uploaded the GPS data to an online Dropbox site on a daily basis to be accessed for Professional Land Surveyor (PLS) oversight, QA/QC review, and processing. OPUS processing triangulates the monument position using 3 CORS stations resulting in a fully adjusted position. After all data had been collected at each monument, accuracy and error ellipses were calculated from the OPUS reports. This information leads to a rating of the monument based on FGDC-STD-007.2-1998[2] at the 95% confidence level. When a statistically stable position was found CORPSCON[3] 6.0.1 software was used to convert the UTM positions to geodetic positions. This geodetic position was used for processing the LiDAR data.

RTK and aircraft mounted GPS measurements were made during periods with PDOP[4] less than or equal to 3.0 and with at least 6 satellites in view of both a stationary reference receiver and the roving receiver. Static GPS data collected in a continuous session average the high PDOP into the final solution in the method used by CORS stations. RTK positions were collected on bare earth locations such as paved, gravel or stable dirt roads, and other locations where the ground is clearly visible (and is likely to remain visible) from the sky during the data acquisition and RTK measurement period(s). RTK measurements are not taken on highly reflective surfaces such as center line stripes or lane markings on roads. RTK points were taken no closer than one meter to any nearby terrain breaks such as road edges or drop offs.

[2] Federal Geographic Data Committee Draft Geospatial Positioning Accuracy Standards (Part 2 table 2.1)
[3] U.S. Army Corps of Engineers , Engineer Research and Development Center Topographic Engineering Center software
[4]PDOP: Point Dilution of Precision is a measure of satellite geometry, the smaller the number the better the geometry between the point and the satellites.

Figure 2. RTK and base station locations used for the Battle Creek LiDAR survey

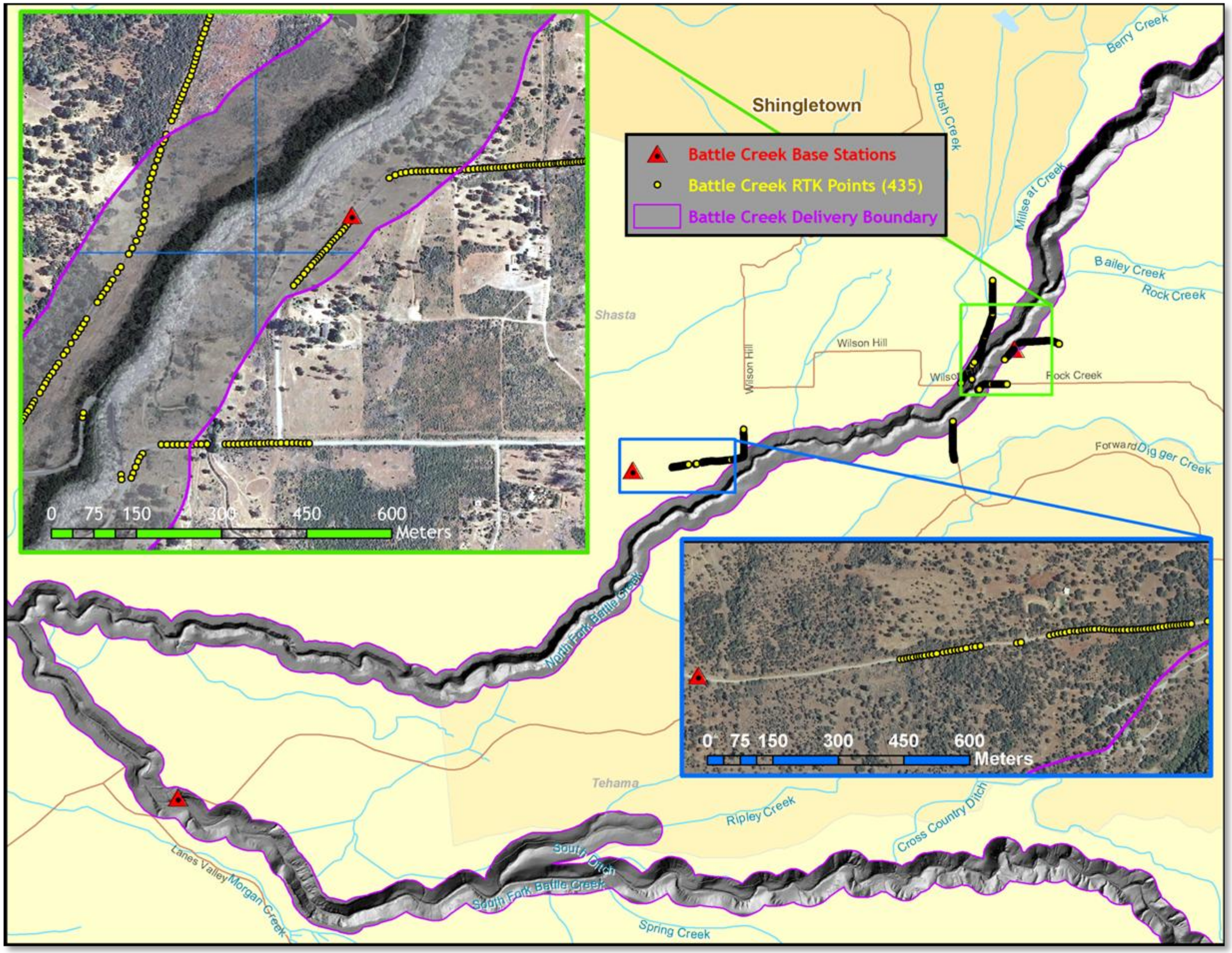

3. Data Processing

3.1 Applications and Work Flow Overview

1. Resolved kinematic corrections for aircraft position data using kinematic aircraft GPS and static ground GPS data.

   Software: Waypoint GPS v.8.10, Trimble Geomatics Office v.1.62

2. Developed a smoothed best estimate of trajectory (SBET) file that blends post-processed aircraft position with attitude data Sensor head position and attitude were calculated throughout the survey. The SBET data were used extensively for laser point processing.

   Software: IPAS v.1.35

3. Calculated laser point position by associating SBET position to each laser point return time, scan angle, intensity, etc. Created raw laser point cloud data for the entire survey in *.las (ASPRS v. 1.2) format.

   Software: ALS Post Processing Software v.2.7

4. Imported raw laser points into manageable blocks (less than 500 MB) to perform manual relative accuracy calibration and filter for pits/birds. Ground points were then classified for individual flight lines (to be used for relative accuracy testing and calibration).

   Software: TerraScan v.11.009

5. Using ground classified points per each flight line, the relative accuracy was tested. Automated line-to-line calibrations were then performed for system attitude parameters (pitch, roll, heading), mirror flex (scale) and GPS/IMU drift. Calibrations were performed on ground classified points from paired flight lines. Every flight line was used for relative accuracy calibration.

   Software: TerraMatch v.11.006

6. Position and attitude data were imported. Resulting data were classified as ground and non-ground points. Statistical absolute accuracy was assessed via direct comparisons of ground classified points to ground RTK survey data. Data were then converted to orthometric elevations (NAVD88) by applying a Geoid09 correction.

   Software: TerraScan v.11.009, ArcMap v. 9.3.1, TerraModeler v.11.004

7. Bare Earth models were created as a triangulated surface and exported as ArcInfo ASCII grids at a 1 meter pixel resolution. Highest Hit models were created for any class at 1 meter grid spacing and exported as ArcInfo ASCII grids.

8. Converted raw images to tif format, calibrating raw image pixels for gain and exposure settings of each image.

   Software: Leica Calibration Post Processing v.1.0.4

9. Calculated photo position and orientation by associating the SBET position (Step 3) to each image capture time.

   Software: IPASCO v.1.3

10. Orthorectified calibrated tiffs utilizing photo orientation information (Step 8) and the LiDAR-derived ground surface (Step 6).

    Software: Leica Photogrammetry Suite v.9.2

11. To correct light imbalances between overlapping images, radiometric global tilting adjustments were applied to the rectified images.

    Software: OrthoVista v.4.4.

12. The color corrected images were then mosaicked together for the survey area and subset into tiles to make the file size more manageable.

    Software: OrthoVista v.4.4.

13. Mosaicked tiles were inspected for misalignments introduced by automatic seam generation. Misalignments were corrected by manual adjustments to seams.

    Software: Adobe Photoshop 7.0, OrthoVista v.4.4.

3.2 Aircraft Kinematic GPS and IMU Data

LiDAR survey datasets were referenced to the 1 Hz static ground GPS data collected over pre-surveyed monuments with known coordinates. While surveying, the aircraft collected 2 Hz kinematic GPS data, and the onboard inertial measurement unit (IMU) collected 200 Hz aircraft attitude data. Leica IPAS Suite was used to process the kinematic corrections for the aircraft. The static and kinematic GPS data were then post-processed after the survey to obtain an accurate GPS solution and aircraft positions. Waypoint was used to develop a trajectory file that includes corrected aircraft position and attitude information. The trajectory data for the entire flight survey session were incorporated into a final smoothed best estimated trajectory (SBET) file that contains accurate and continuous aircraft positions and attitudes.

3.3 Laser Point Processing

Laser point coordinates were computed using the IPAS and ALS Post Processor software suites based on independent data from the LiDAR system (pulse tim, scan angle), and aircraft trajectory data (SBET). Laser point returns (first through fourth) were assigned an associated (x, y, z) coordinate along with unique intensity values (0-255). The data were output into large LAS v. 1.2 files; each point maintains the corresponding scan angle, return number (echo), intensity, and x, y, z (easting, northing, and elevation) information.

These initial laser point files were too large for subsequent processing. To facilitate laser point processing, bins (polygons) were created to divide the dataset into manageable sizes (< 500 MB). Flightlines and LiDAR data were then reviewed to ensure complete coverage of the survey area and positional accuracy of the laser points.

Laser point data were imported into processing bins in TerraScan, and manual calibration was performed to assess the system offsets for pitch, roll, heading and scale (mirror flex). Using a geometric relationship developed by Watershed Sciences, each of these offsets was resolved and corrected if necessary.

LiDAR points were filtered for noise, pits (artificial low points), and birds (true birds as well as erroneously high points) by screening for absolute elevation limits, isolated points and height above ground. Each bin was then manually inspected for remaining pits and birds and spurious points were removed. In a bin containing approximately 7.5-9.0 million points, an average of 50-100 points are typically found to be artificially low or high. Common sources of non-terrestrial returns are clouds, birds, vapor, haze, decks, brush piles, etc.

Internal calibration was refined using TerraMatch. Points from overlapping lines were tested for internal consistency and final adjustments were made for system misalignments (i.e., pitch, roll, heading offsets and scale). Automated sensor attitude and scale corrections yielded 3-5 cm improvements in the relative accuracy. Once system misalignments were corrected, vertical GPS drift was then resolved and removed per flight line, yielding a slight improvement (<1 cm) in relative accuracy.

The TerraScan software suite is designed specifically for classifying near-ground points (Soininen, 2004). The processing sequence began by 'removing' all points that were not 'near' the earth based on geometric constraints used to evaluate multi-return points. The resulting bare earth (ground) model was visually inspected and additional ground point modeling was performed in site-specific areas to improve ground detail. This manual editing of grounds often occurs in areas with known ground modeling deficiencies, such as: bedrock outcrops, cliffs, deeply incised stream banks, and dense vegetation. In some cases, automated ground point classification erroneously included known vegetation (i.e., understory, low/dense shrubs, etc.). These points were manually reclassified as non-grounds. Ground surface rasters were developed from triangulated irregular networks (TINs) of ground points.

3.4 Orthophotograph Processing

Image radiometric values were calibrated to specific gain and exposure settings associated with each capture using Leica's Calibration Post Processing software. The calibrated images were saved in tiff format to be used as inputs for the rectification process.
Photo position and orientation was then calculated by assigning aircraft position and attitude information to each image by associating the time of image capture with trajectory file (SBET) in IPASCO. Photos were then orthorectified to the LiDAR derived ground surface using LPS. This typically results in <3 pixel relative accuracy between images. Relative accuracy can vary slightly with terrain but offsets greater than 3 pixels tend to manifest at the image edges which are typically removed in the mosaic process.

The rectified images were mosaicked together in a three step process using Orthovista. First, color correction was applied to each image using global tilting adjustments designed to homogenize overlapping regions. Second, an automated seam generation process selected the most nadir portion of each image while drawing seams around landscape features such that discrepancies between images were minimized. Finally, the mosaic was subset into the 500 m x 500 m tiling structure.

3.5 Contour Development

Contour lines were derived at 0.5 meter minor intervals and 2 meter major intervals from ground-classified LiDAR point data using TerraSolid processing software in MicroStation v. 8.01.02.15 Contour generation from LiDAR point data requires a thinning operation in order to reduce contour sinuosity. Parameters for these operations are: thinning elevation bounds: +/- 0.07m; search radius: 6.09m. The thinning operation reduces point density where topographic change is minimal (flat surfaces) while preserving resolution where topographic change is present. The total sum of potential error in vertical position is equal to twice the point processing limits (0.14m) plus twice the 2-sigma absolute vertical accuracy value for this dataset.

Ground point density rasters were created within MicroStation using a 1 meter step resolution and a 2 meter sampling radius. Areas with less than 0.25 ground-classified points per square meter were considered "sparse" and areas with higher densities were considered "covered". The ground point density raster data are in ESRI GRID format and have a 1 meter pixel resolution. The contour lines were intersected with ground point density raster data, allowing the addition of a confidence attribute to contour lines. Contour lines over "sparse" areas have low confidence, while contour lines over "covered" areas have a high confidence. Areas with low ground point density are commonly beneath buildings and bridges, in locations with dense vegetation, over water, and in other areas where laser penetration to the ground surface is impeded. **Figure 3** is an example of a ground point density raster and contour lines.

Figure 3. *Elevation contours over LiDAR ground-classified point density raster (left) and true-color aerial photograph (right). Red indicates low ground point density and blue represents high density.*

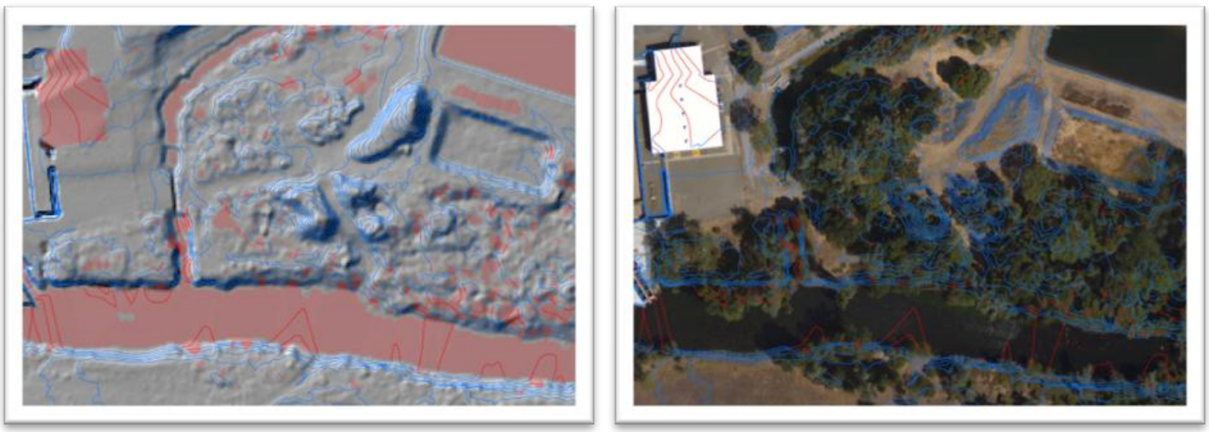

3.5 Hydro Flattened & Breakline Enforced Terrain Models

David C. Smith and Associates (DSA), Portland, OR created breaklines for the Battle Creek study area using LiDAR-grammetry. **Table 2** describes the type and definition of each breakline collected. The breaklines were used to supplement the LiDAR data in creation of a hydro-flattened/hydro-enforced ground model. A breakline was created around lakes and ponds with areas larger than ~2 acres. Rivers with widths greater than 3 meters were represented as a double line feature and flatten from side-to-side. A single line feature was used to represent streams less than ~3 meters.

- Water boundaries were enforced using hard breaklines and water surfaces were flattened based on the elevation from the breaklines. The breakline boundaries were also used to reassign any ground classified points within the water delineated areas to a water class.
- Hard breaklines (stream edges, islands, etc.) were incorporated into the TIN by enforcing triangle edges (adjacent to the breakline) to the elevation values derived from the LiDAR-grammetric breakline. This implementation corrected interpolation along the hard edge.
- Culverts and artificial impediments to drainage flow were identified with hard breaklines. LiDAR data points within one meter of a culvert breakline were ignored from the ground classification, giving precedence to breakline Z values. This enforces proper drainage flow in development of the ground model.
- ArcHydro Tools 9 was run on resulting ground models as a quality inspection of stream definition. In areas where stream definition deviated from bare earth ground model

and breaklines, LiDAR data was reexamined to provide increased detail (adding or subtracting appropriate ground classified points).

***Table 2**. Breaklines collected for the Battle Creek study area.*

Feature	Implementation	Description
Water Lake	Hard Breakline	Lake Bodies
Water Stream	Hard Breakline	Streams wider than ~3 meters
Water Island	Hard Breakline	Islands
Culvert Breakline	Hard Breakline	High Confidence breakline through culvert
Culvert Connector	Hard Breakline	Low Confidence breakline through culvert
Breakline	Hard Breakline	High Confidence breakline to supplement LiDAR data
Breakline Obscured	Hard Breakline	Low confidence breakline to supplement LiDAR data

***Figure 4**. Left: LiDAR bare earth model before hydro-enforcement/hydro-flattening. Right: LiDAR bare earth hydro-enforced/hydro-flattened model with breaklines (blue: Water Stream, orange: Culvert Breakline).*

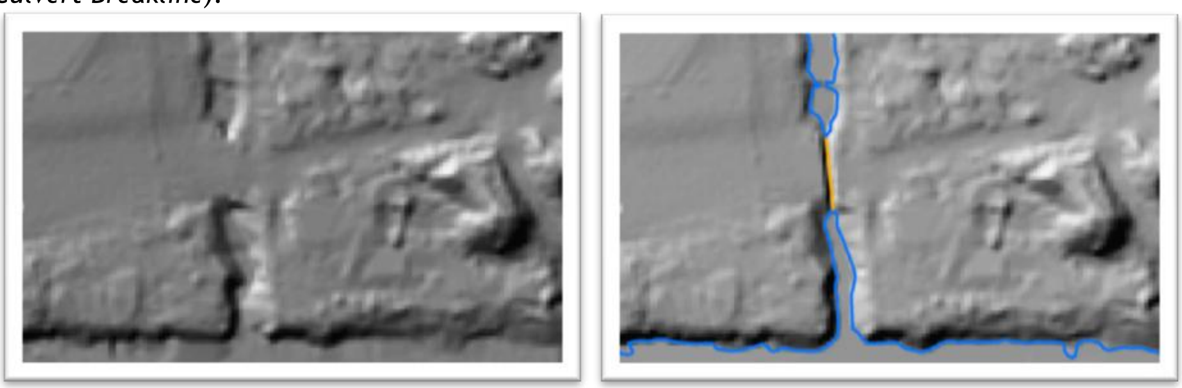

4. LiDAR Accuracy Assessment

4.1 Laser Noise and Relative Accuracy

Laser Noise

For any given target, laser noise is the breadth of the data cloud per laser return (i.e., last, first, etc.). Lower intensity surfaces (roads, rooftops, still/calm water) experience higher laser noise. The laser noise range for this survey was approximately 0.02 meters.

Relative Accuracy

Relative accuracy refers to the internal consistency of the data set - the ability to place a laser point in the same location over multiple flight lines, GPS conditions, and aircraft attitudes. Affected by system attitude offsets, scale, and GPS/IMU drift, internal consistency is measured as the divergence between points from different flight lines within an overlapping area. Divergence is most apparent when flight lines are opposing. When the

LiDAR system is well calibrated, the line-to-line divergence is low (<10 cm). See Appendix A for further information on sources of error and operational measures that can be taken to improve relative accuracy.

Relative Accuracy Calibration Methodology

1. Manual System Calibration: Calibration procedures for each mission require solving geometric relationships that relate measured swath-to-swath deviations to misalignments of system attitude parameters. Corrected scale, pitch, roll and heading offsets were calculated and applied to resolve misalignments. The raw divergence between lines was computed after the manual calibration was completed and reported for each survey area.
2. Automated Attitude Calibration: All data were tested and calibrated using TerraMatch automated sampling routines. Ground points were classified for each individual flight line and used for line-to-line testing. System misalignment offsets (pitch, roll and heading) and scale were solved for each individual mission and applied to respective mission datasets. The data from each mission were then blended when imported together to form the entire area of interest.
3. Automated Z Calibration: Ground points per line were utilized to calculate the vertical divergence between lines caused by vertical GPS drift. Automated Z calibration was the final step employed for relative accuracy calibration.

4.2 Absolute Accuracy

To minimize the contributions of laser noise and relative accuracy to absolute error, a number of noise filtering and calibration procedures were performed prior to evaluating absolute accuracy. The LiDAR quality assurance process uses the data from the real-time kinematic (RTK) ground survey conducted in the AOI. For the Battle Creek survey area, a total of **435** RTK GPS measurements were collected. All measurements were collected on hard surfaces and distributed among multiple flight swaths. To assess absolute accuracy the location coordinates of these known RTK ground points were compared to those calculated for the closest ground-classified laser points.

The vertical accuracy of the LiDAR data is described as the mean and standard deviation (sigma ~1σ) of divergence of LiDAR point coordinates from RTK ground survey point coordinates. To provide a sense of the model predictive power of the dataset, the root mean square error (RMSE) for vertical accuracy is also provided. These statistics assume the error distributions for x, y, and z are normally distributed, thus the skew and kurtosis of distributions when evaluating error statistics is considered.

Statements of statistical accuracy apply to fixed terrestrial surfaces only and may not be applied to areas of dense vegetation or steep terrain (See Appendix A).

5. Photo Accuracy Assessment

To assess spatial accuracy of the orthophotographs they are compared against checkpoints identified from the LIDAR intensity images. The checkpoints were measured on surface features such as painted road-lines and fixed high contrast objects on the ground surface. RTK checkpoints were also collected in locations where the ground is clearly visible from the sky during acquisition. The accuracy of the final mosaic, expressed as root mean square error (RMSE), was calculated in relation to the RTK positions and LiDAR-derived control points. The accuracy of the final mosaic, expressed as root mean square error (RMSE), was calculated in relation to the LiDAR-derived checkpoints. **Figure 3** displays the co-registration between orthorectified photographs and LiDAR intensity images.

Figure 5. *Example of co-registration of color images with LiDAR intensity images.*

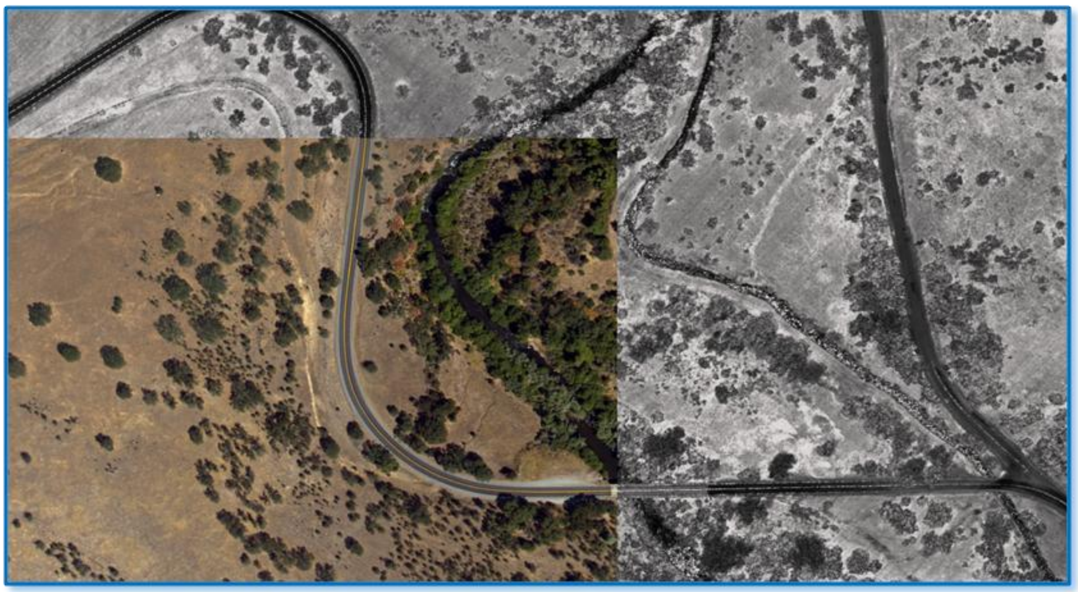

6. Study Area Results

Summary statistics for point resolution and accuracy (relative and absolute) of the LiDAR data collected in the Battle Creek survey area are presented below in terms of central tendency, variation around the mean, and the spatial distribution of the data (for point resolution by tile).

6.1 Data Summary

Table 3. *Resolution and Accuracy - Specifications and Achieved Values*

	Targeted	Achieved

Resolution:	≥ 8 points/m^2	9.13 points/m^2
Vertical Accuracy (1 σ):	<15 cm	2.1 cm

6.2 Data Density/Resolution

Certain types of surfaces (e.g. water, dense vegetation, breaks in terrain, steep slopes) may return fewer pulses (delivered density) than the laser originally emitted (native density).

Ground classifications were derived from automated ground surface modeling and manual, supervised classifications where it was determined that the automated model had failed. Ground-classified return densities will be lower in areas of dense vegetation, water, or buildings. **Figures 8-9** display the distribution of average first-return and ground-classified point densities by processing tile.

Data Resolution for the Battle Creek survey area (***meters***):

- Average Point (First Return) Density = **9.13 points/m^2**
- Average Ground Point Density = **2.59 points/m^2**

Figure 6. *Density distribution for first return laser points*

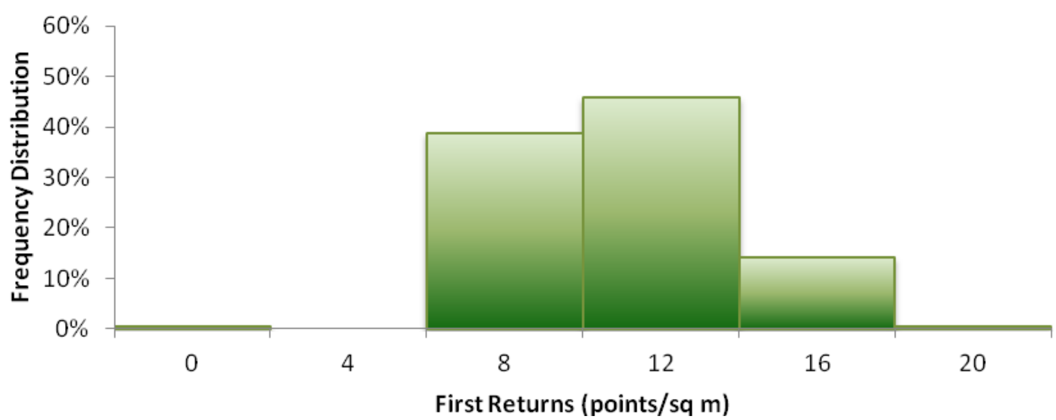

Figure 7. *Density distribution for ground-classified laser points*

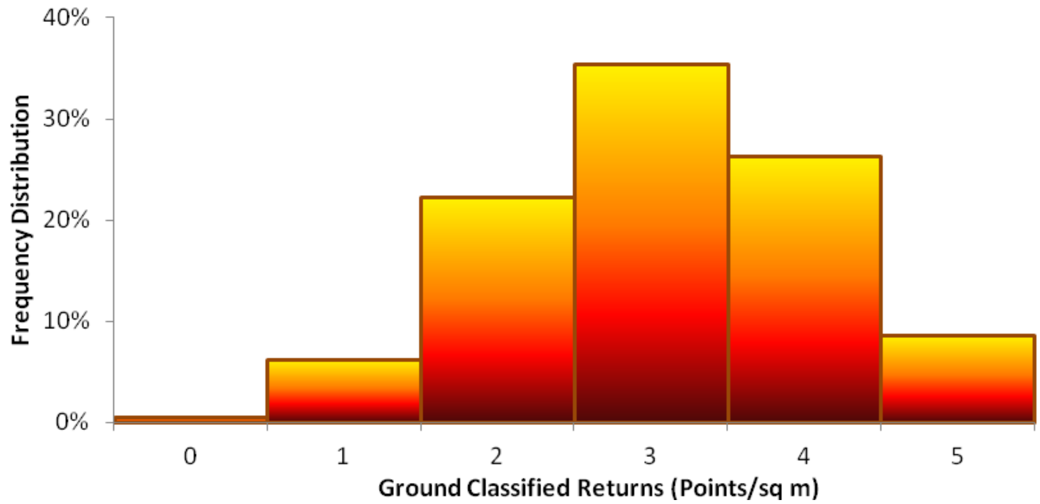
40%
30%
20%
10%
0%
Frequency Distribution
0
1
2
3
4
5
Ground Classified Returns (Points/sq m)

Figure 8. *First Return laser point data density per tile for the 2011 Battle Creek survey (meters)*

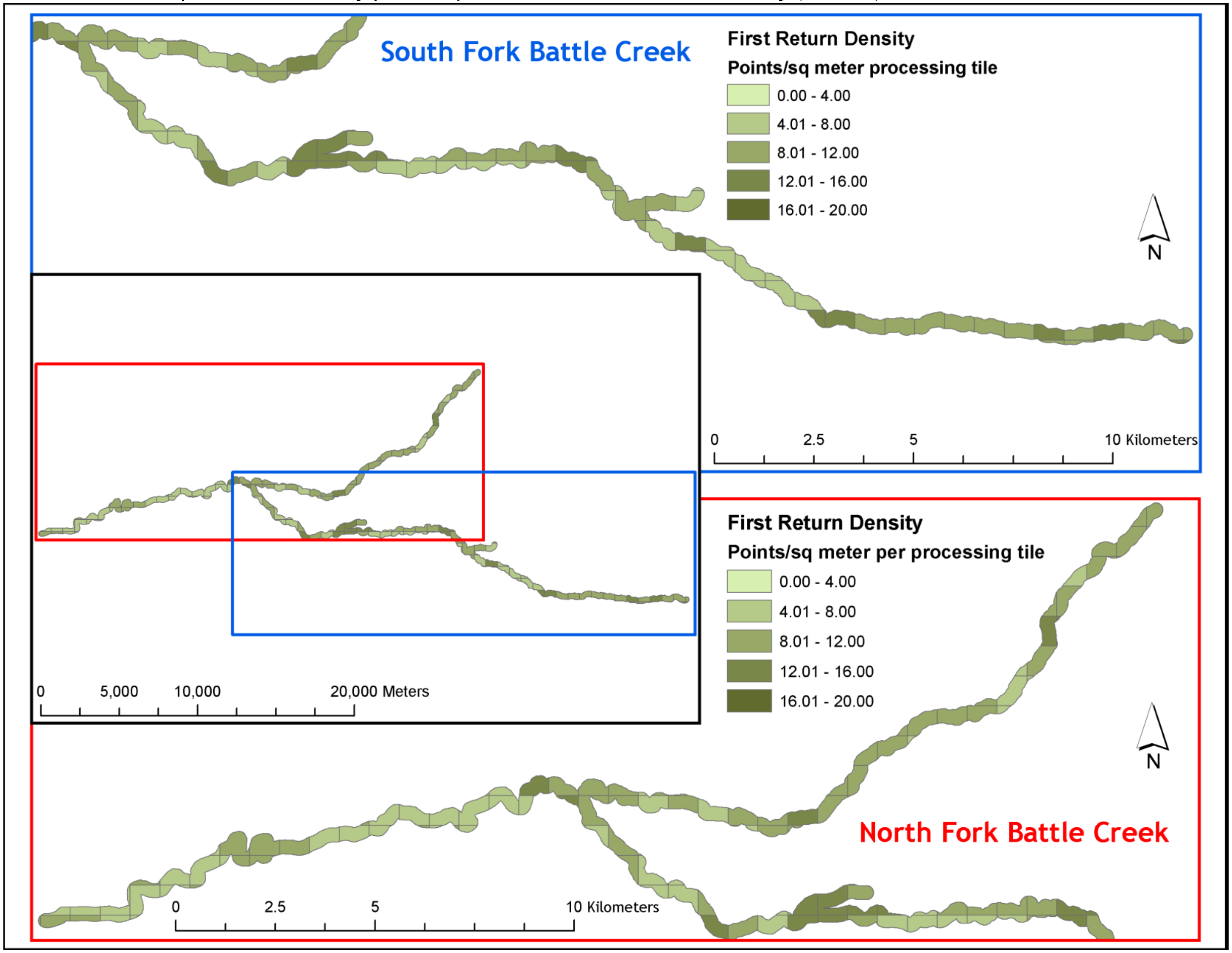

Figure 9*. Ground Return laser point data density per tile for the 2011 Battle Creek survey (Meters)*

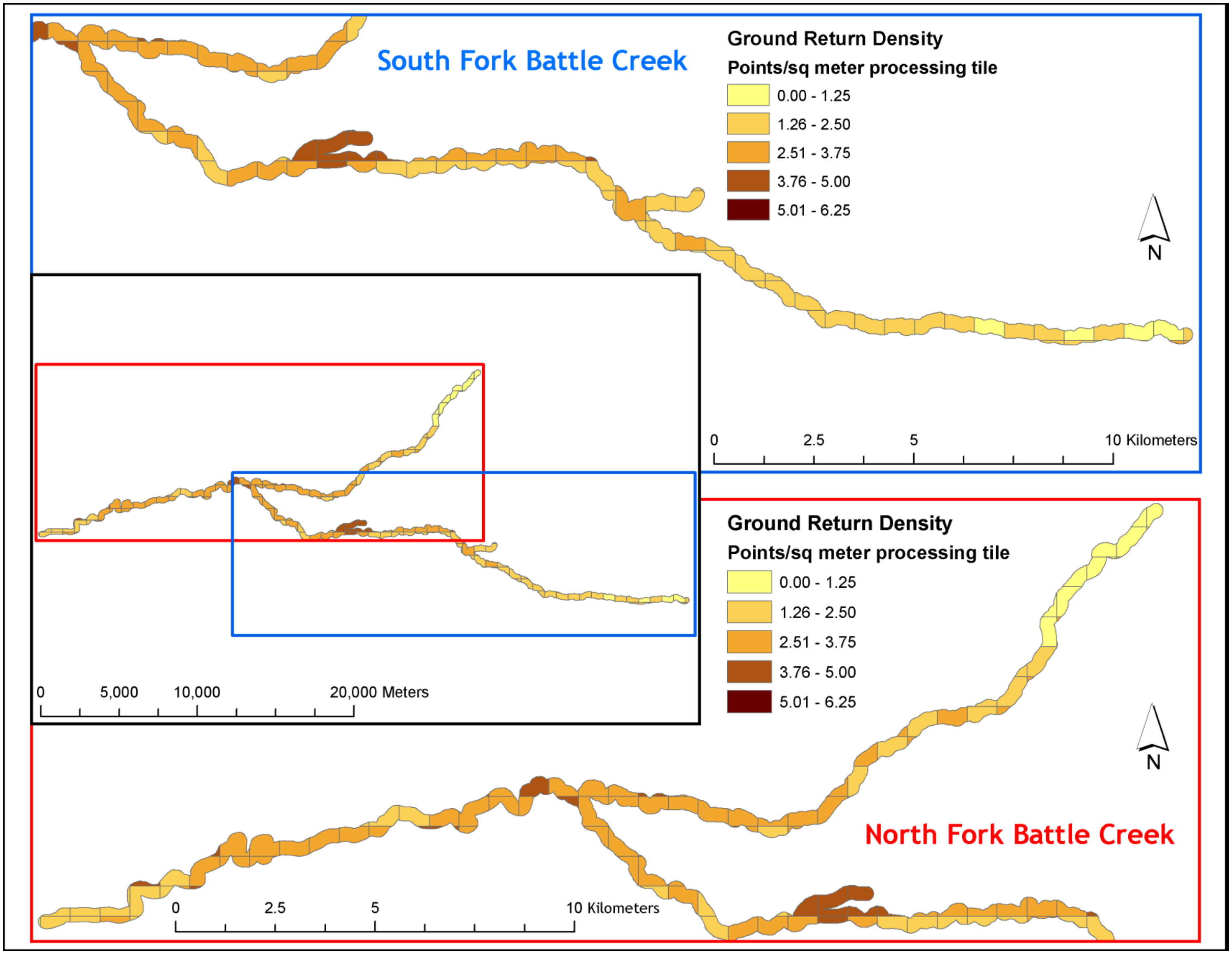
South Fork Battle Creek
Ground Return Density
Points/sq meter processing tile
0.00 - 1.25
1.26 - 2.50
2.51 - 3.75
3.76 - 5.00
5.01 - 6.25
N
0
2.5
5
10 Kilometers
0
5,000
10,000
20,000 Meters
Ground Return Density
Points/sq meter processing tile
0.00 - 1.25
1.26 - 2.50
2.51 - 3.75
3.76 - 5.00
5.01 - 6.25
N
North Fork Battle Creek
0
2.5
5
10 Kilometers

6.3 Relative Accuracy Calibration Results

Relative accuracies for the Battle Creek survey area measure the full survey calibration including areas outside the delivered boundary:

- Project Average = 0.06 m
- Median Relative Accuracy = 0.03 m
- 1σ Relative Accuracy = 0.01 m
- 1.96σ Relative Accuracy = 0.02 m

Figure 10. *Distribution of relative accuracies per flight line, non slope-adjusted*

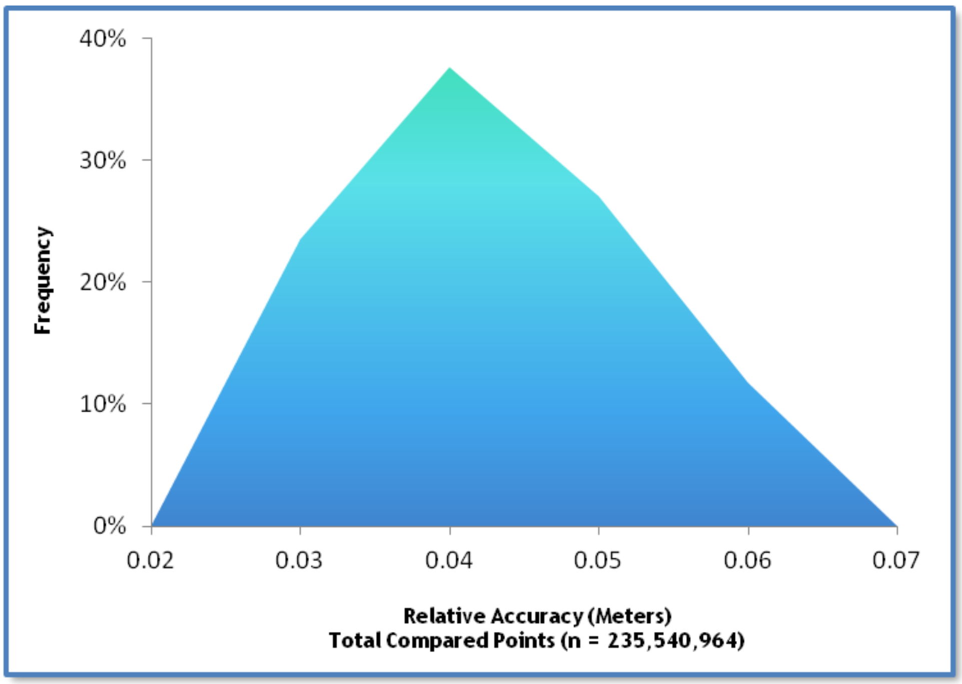

6.4 Absolute Accuracy

Absolute accuracies for the Battle Creek Survey Area

Table 4. *Absolute Accuracy – Deviation between laser points and RTK hard surface survey points*

RTK Survey Sample Size (n): 435		
Root Mean Square Error (RMSE) = 0.02 m		Minimum Δz = -0.08 m
Standard Deviations:		Maximum Δz = 0.05 m
1 sigma (σ) = 0.02 m	1.96 sigma (σ) = 0.04 m	Average Δz = -0.006 m

Figure 11. Absolute Accuracy - Histogram Statistics, based on 435 hard surface points

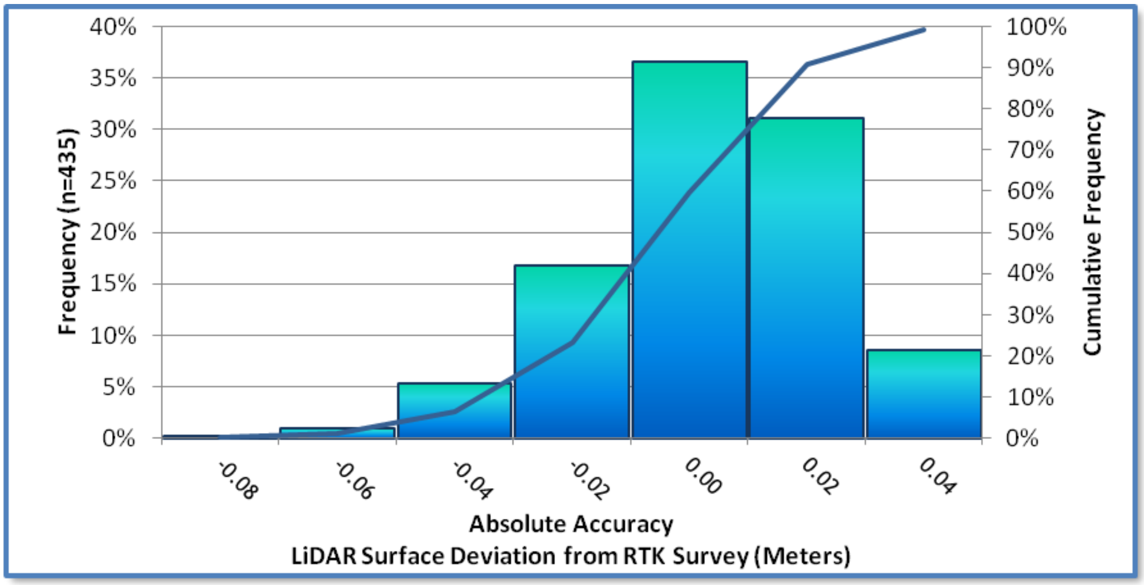

6.5 Photo Accuracy

***Figure 12**. Orthophotographs for the Battle Creek survey area displayed with accuracy checkpoints identified from the LiDAR intensity images.*

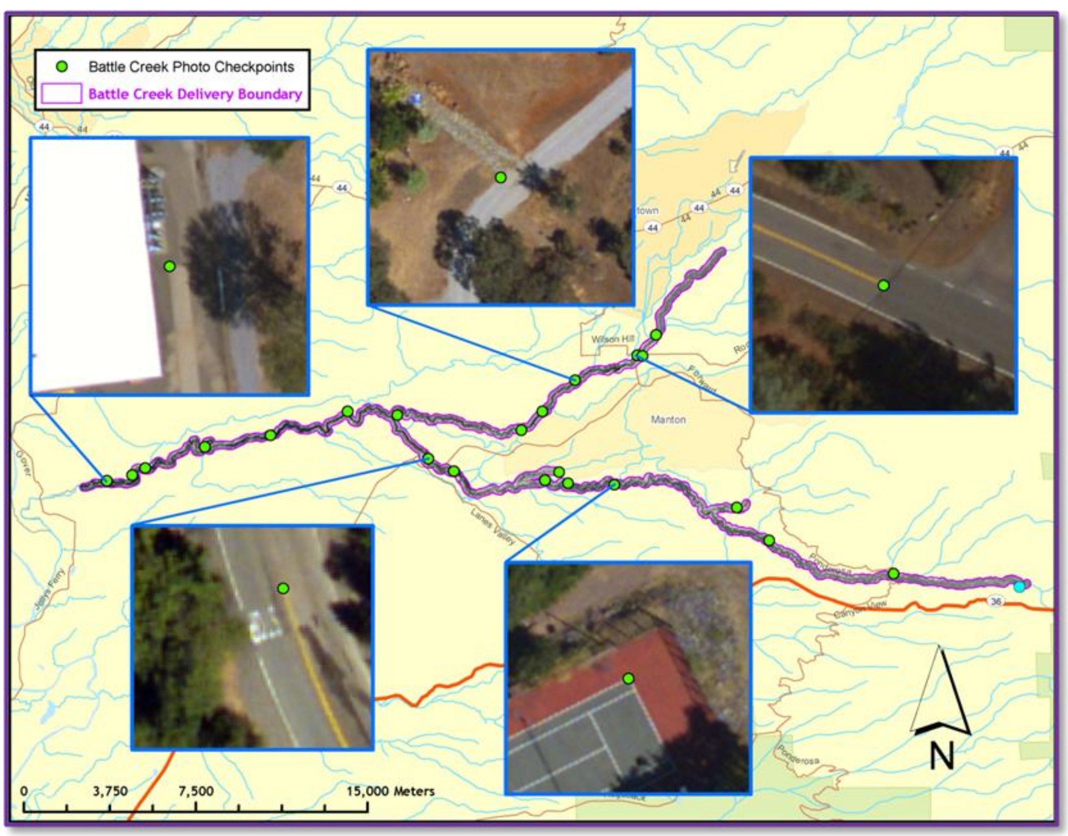

Figure 13. *Orthophotographs for the Battle Creek survey area displayed with air target RTK accuracy checkpoints*

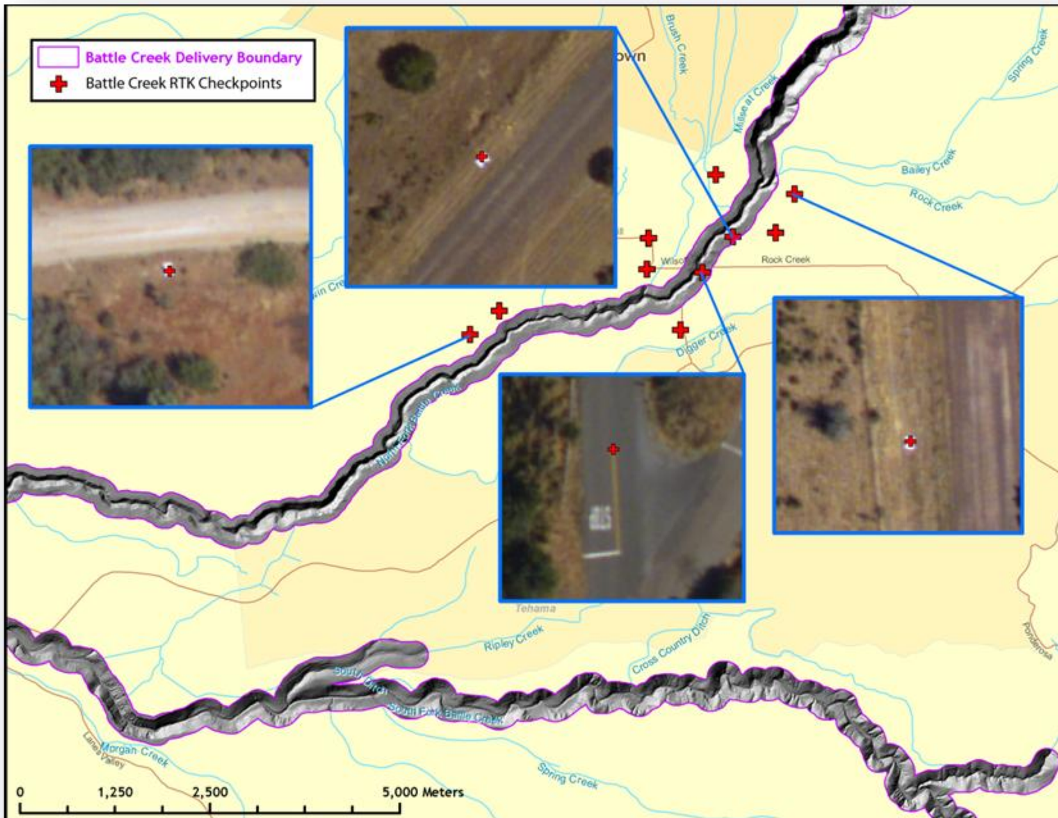

Table 5. *Deviation between aerial photos and intensity images*

	Mean	Standard Deviation (1 Sigma)	Root Mean Square Error (RMSE)
Battle Creek Photos	0.09 m	0.46 m	0.46 m

Figure 14. *Checkpoint residuals derived from comparing aerial photos to intensity images*

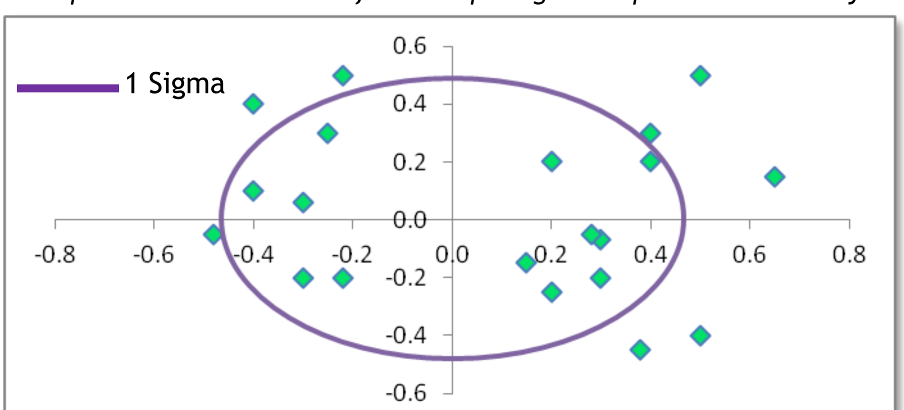

7. Projection/Datum and Units

Battle Creek		
Projection:		UTM Zone 10
Datum	Vertical:	NAVD88 Geoid09
	Horizontal:	NAD83 (HARN)
Units:		Meters

8. Deliverables

Battle Creek	

Point Data:	• LAS v.1.2 format
	    • All laser returns with adjusted GPS time
	    • Ground returns with adjusted GPS time

Vector Data:	• Survey boundary (ESRI shapefile format) • LiDAR Index (ESRI shapefile format) • Ortho Index (ESRI shapefile format) • DEM Index (ESRI shapefile format)

Raster Data:	• Elevation models (ESRI GRID format , 1 meter resolution):
	    • Bare Earth Model
	    • Highest Hit Model
	• Intensity images (GeoTIFF format,0.5 meter resolution)

Orthophotos	• True-Color Orthophotos (GeoTIFF format, 20 cm resolution, MrSID Full Mosaic)
Data Report:	• Full report containing introduction, methodology, and accuracy for the Battle Creek survey area.

9. Selected Images

Figure 14. *Overhead view of the Coleman Fish Hatchery along Battle Creek. Image was created using 2011 orthophotos draped over the 2011 LiDAR intensity image mosaic and highest hit hillshade.*

Figure 15*. This is an overhead view of the confluence of North & South Battle Creek, and the Pacific Gas and Electric Coleman Canal. Image was created using 2011 orthophotos draped over the 2011 LiDAR intensity image mosaic and highest hit hillshade.*

***Figure 16**. Image is looking north at several sharp bends in Battle Creek just south of the Coleman Fish Hatchery Road. Image is a 3D point cloud colored by 2011 orthophotos.*

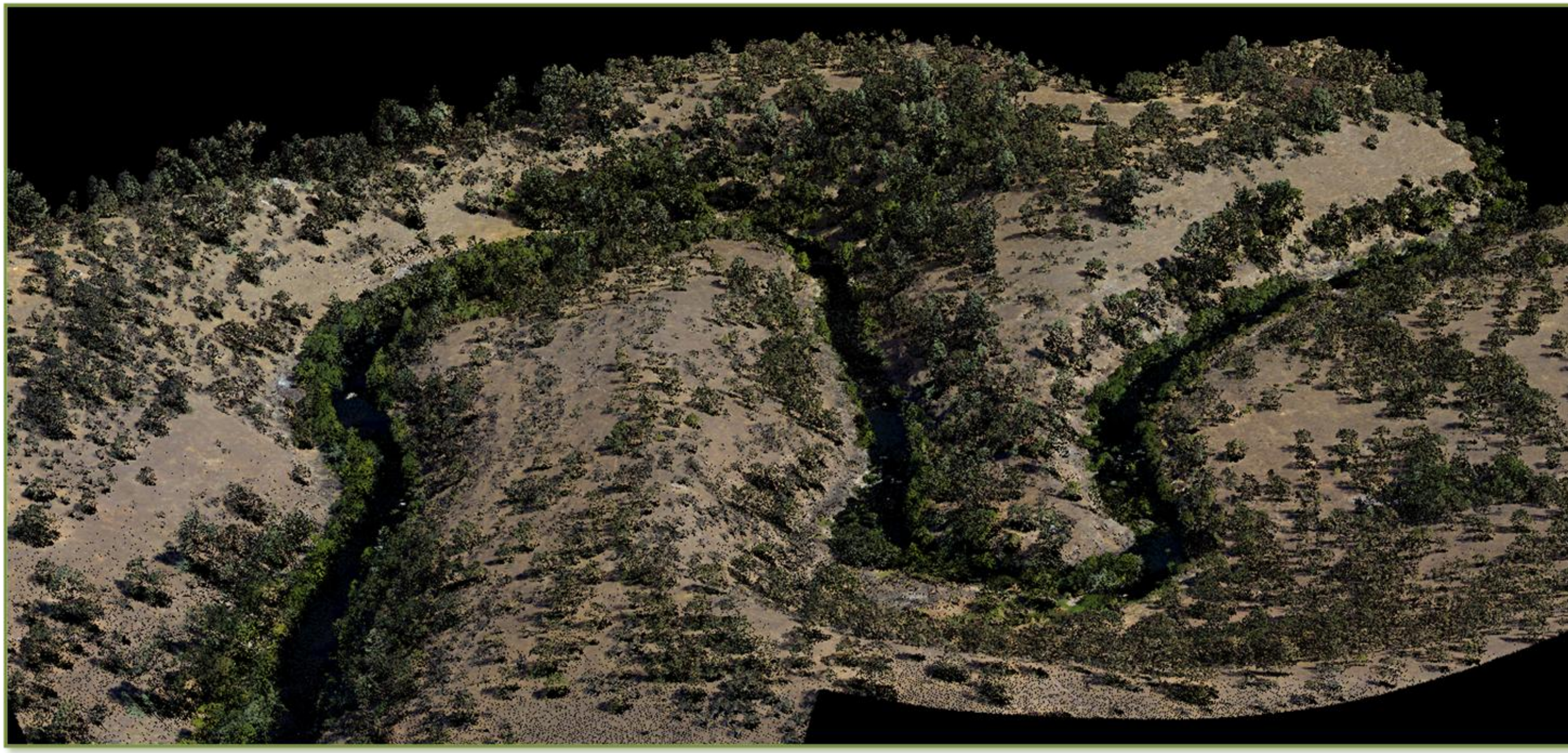

Figure 17. *Image is looking southeast at a dam and power station along South Battle Creek east of Spencer Lake Road. Image is a 3D point cloud colored by 2011 orthophotos.*

***Figure 18**. Image is looking northeast at power lines crossing over South Battle Creek just south of Spencer Lake Road. Image was created using 2011 orthophotos draped over a 3D LiDAR point cloud.*

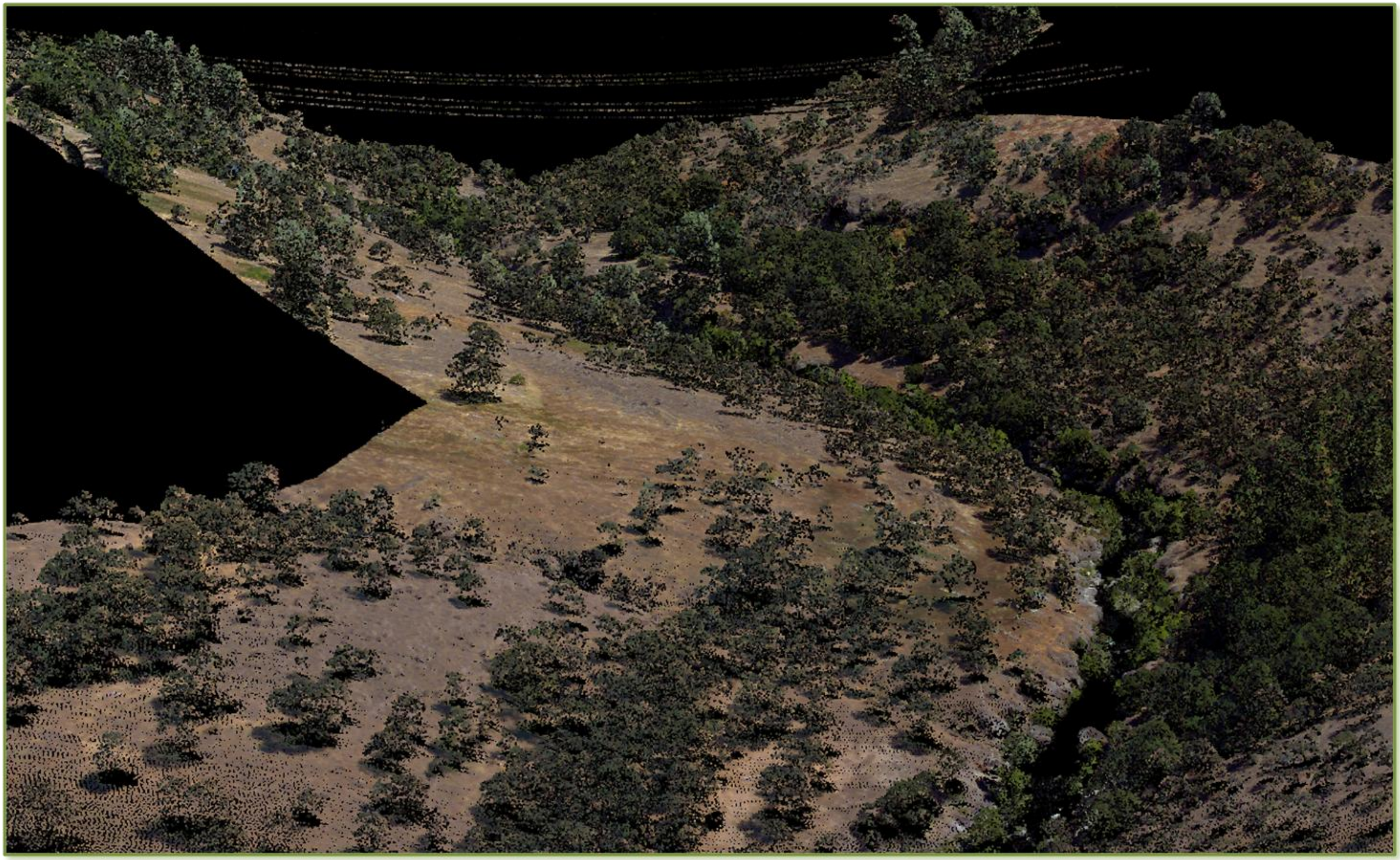

10. Glossary

1-sigma (σ) Absolute Deviation: Value for which the data are within one standard deviation (approximately 68th percentile) of a normally distributed data set.
2-sigma (σ) Absolute Deviation: Value for which the data are within two standard deviations (approximately 95th percentile) of a normally distributed data set.
Root Mean Square Error (RMSE): A statistic used to approximate the difference between real-world points and the LiDAR points. It is calculated by squaring all the values, then taking the average of the squares and taking the square root of the average.
Pulse Rate (PR): The rate at which laser pulses are emitted from the sensor; typically measured as thousands of pulses per second (kHz).
Pulse Returns: For every laser pulse emitted, the Leica ALS 50 Phase II system can record *up to four* wave forms reflected back to the sensor. Portions of the wave form that return earliest are the highest element in multi-tiered surfaces such as vegetation. Portions of the wave form that return last are the lowest element in multi-tiered surfaces.
Accuracy: The statistical comparison between known (surveyed) points and laser points. Typically measured as the standard deviation (sigma, σ) and root mean square error (RMSE).
Intensity Values: The peak power ratio of the laser return to the emitted laser. It is a function of surface reflectivity.
Data Density: A common measure of LiDAR resolution, measured as points per square meter.
Spot Spacing: Also a measure of LiDAR resolution, measured as the average distance between laser points.
Nadir: A single point or locus of points on the surface of the earth directly below a sensor as it progresses along its flight line.
Scan Angle: The angle from nadir to the edge of the scan, measured in degrees. Laser point accuracy typically decreases as scan angles increase.
Overlap: The area shared between flight lines, typically measured in percents; 100% overlap is essential to ensure complete coverage and reduce laser shadows.
DTM / DEM: These often-interchanged terms refer to models made from laser points. The digital elevation model (DEM) refers to all surfaces, including bare ground and vegetation, while the digital terrain model (DTM) refers only to those points classified as ground.
Real-Time Kinematic (RTK) Survey: GPS surveying is conducted with a GPS base station deployed over a known monument with a radio connection to a GPS rover. Both the base station and rover receive differential GPS data and the baseline correction is solved between the two. This type of ground survey is accurate to 1.5 cm or less.

11. Citations

Soininen, A. 2004. TerraScan User's Guide. TerraSolid.

Appendix A

LiDAR accuracy error sources and solutions:

Type of Error	Source	Post Processing Solution
GPS (Static/Kinematic)	Long Base Lines	None
	Poor Satellite Constellation	None
	Poor Antenna Visibility	Reduce Visibility Mask
Relative Accuracy	Poor System Calibration	Recalibrate IMU and sensor offsets/settings
	Inaccurate System	None
Laser Noise	Poor Laser Timing	None
	Poor Laser Reception	None
	Poor Laser Power	None
	Irregular Laser Shape	None

Operational measures taken to improve relative accuracy:
Low Flight Altitude: Terrain following is employed to maintain a constant above ground level (AGL). Laser horizontal errors are a function of flight altitude above ground (i.e., ~ 1/3000th AGL flight altitude).
Focus Laser Power at narrow beam footprint: A laser return must be received by the system above a power threshold to accurately record a measurement. The strength of the laser return is a function of laser emission power, laser footprint, flight altitude and the reflectivity of the target. While surface reflectivity cannot be controlled, laser power can be increased and low flight altitudes can be maintained.
Reduced Scan Angle: Edge-of-scan data can become inaccurate. The scan angle was reduced to a maximum of $\pm 14^{o}$ from nadir, creating a narrow swath width and greatly reducing laser shadows from trees and buildings.
Quality GPS: Flights took place during optimal GPS conditions (e.g., 6 or more satellites and PDOP [Position Dilution of Precision] less than 3.0). Before each flight, the PDOP was determined for the survey day. During all flight times, a dual frequency DGPS base station recording at 1–second epochs was utilized and a maximum baseline length between the aircraft and the control points was less than 19 km (11.5 miles) at all times.
Ground Survey: Ground survey point accuracy (i.e. <1.5 cm RMSE) occurs during optimal PDOP ranges and targets a minimal baseline distance of 4 miles between GPS rover and base. Robust statistics are, in part, a function of sample size (n) and distribution. Ground survey RTK points are distributed to the extent possible throughout multiple flight lines and across the survey area.
50% Side-Lap (100% Overlap): Overlapping areas are optimized for relative accuracy testing. Laser shadowing is minimized to help increase target acquisition from multiple scan angles. Ideally, with a 50% side-lap, the most nadir portion of one flight line coincides with the edge (least nadir) portion of overlapping flight lines. A minimum of 50% side-lap with terrain-followed acquisition prevents data gaps.
Opposing Flight Lines: All overlapping flight lines are opposing. Pitch, roll and heading errors are amplified by a factor of two relative to the adjacent flight line(s), making misalignments easier to detect and resolve.